

1 **IL-13 mediates collagen deposition via STAT6 and** 2 **microRNA-135b: a role for epigenetics**

3 Steven O'Reilly^{1*}, Marzena Ciechomska^{2,4,5}, Nicola Fullard³, Stefan Przyborski³, Jacob M. van Laar⁶

4 ¹Faculty of Health and Life Sciences

5 Northumbria University

6 Newcastle Upon Tyne

7 NE3 3YH

8 United Kingdom

9 ²Institute of Cellular Medicine

10 Faculty of Medical Sciences

11 MRG 4th Floor Cookson Building

12 Framlington Place

13 Newcastle Upon Tyne

14 NE2 4HH

15 ³School of Biomedical Science,

16 Durham University

17 Durham

18 United Kingdom

19 ⁴Institute of Immunology and Experimental Therapy, Polish Academy of Science, Wroclaw, Poland

20 ⁵The National Institute of geriatrics rheumatology and rehabilitation, Warsaw, Poland

21 ⁶Department of Rheumatology and Clinical Immunology

22 University Medical Centre Utrecht

23 Utrecht

24 The Netherlands

- 25
- 26 • Address for correspondence: Steven O'Reilly PhD Faculty of Health and Life Sciences,
27 Northumbria University, Newcastle Upon Tyne, United Kingdom
28 steven.oreilly@northumbria.ac.uk Telephone; +44 01914911530

32
33
34
35
36
37
38
39
40
41
42
43
44
45
46
47
48
49
50
51
52
53
54
55
56
57
58
59
60
61
62
63
64
65
66
67

Abstract

Systemic sclerosis is an autoimmune connective tissue disease in which T cells play a prominent role. We and others have previously demonstrated a role for T cell-derived IL-13 in mediating the induction of collagen in dermal fibroblasts and that blockade with IL-13 antibodies attenuates this increase. In this study we want to probe the signalling that underpins IL-13 mediated matrix deposition. Isolated dermal fibroblasts were incubated with recombinant IL-13 and gene expression by qRT-PCR was performed for collagen1A1 and TGF- β 1. Small interfering RNA (siRNA) was used to knock down STAT6 and a small molecule inhibitor was also used to block this pathway. MiR-135b was transfected into fibroblasts plus and minus IL-13 to see if this miR plays a role. miR-135b was measured in systemic sclerosis fibroblasts isolated from patients and also in serum. Results showed that IL-13 increased collagen expression and that this is independent from TGF- β 1. This is dependent on STAT6 as targeting this blocked induction. MiR-135b reduces collagen induction in fibroblasts and scleroderma fibroblasts have lower constitutive levels of the miR. We further demonstrate that miR135b is repressed by methylation and may include MeCP2. In conclusion we show that STAT6 and miR-135b regulate IL-13-mediated collagen production by fibroblasts.

68
69
70
71
72
73
74
75
76
77
78
79
80
81
82
83
84
85
86
87
88
89
90
91
92
93
94
95
96
97
98
99
100
101
102
103
104
105
106
107
108
109
110

Introduction

Systemic sclerosis (SSc) is a polygenic, idiopathic connective tissue disease characterised by autoimmunity, vascular damage, inflammation and fibrosis. Activation of quiescent fibroblasts into myofibroblasts that express alpha-smooth muscle actin and secrete excessive extracellular matrix molecules is critical to the fibrosis that underpins the disease pathogenesis¹ and underpins fibrosis whatever organ is affected.

Tissue fibrosis leads to excessive scarring that ultimately leads to loss of organ function and currently there is no disease modifying drug approved for treatment and there is substantial morbidity and mortality. Experimental studies show a clear link between the inflammation and fibrosis and many diverse cell types are involved in the inflammation and fibrosis. It has been shown that monocytes and T cells infiltrate the dermis in SSc especially prominent in early disease. T cells are particularly prominent early in the disease. Activation of T cells has been shown by the expression of T cell activation markers². SSc is characterised by elevated IL-4 and IL-13 levels in serum^{3, 4} and abnormalities in Th2 cells. Indeed there is a correlation between IL-13 serum levels and nailfold capillaroscopy abnormalities in SSc patients⁵. We demonstrated that T cell isolated from skin have upregulated expression of Tumour Necrosis Factor- α (TNF- α) receptors and Interleukin-13 (IL-13)⁶ in SSc patients. Engagement of IL-13 (or IL-4) to its receptor IL-13R and the shared receptor IL-4R α promotes Janus Kinase (JAK) activation that in turn leads to phosphorylation of STAT6, homodimer or heterodimer formation via their amino terminal domains, and translocation to the nucleus where they bind DNA, influencing gene expression in many cell types. STAT6 itself is important for the polarisation of naïve T cells to Th2 effector cells⁷. This activation of STAT6 leads to activation of the transcription factor GATA3 which regulates the expression of Th2 cytokines such as IL-4 and IL-13 thus differentiating the T cells to a Th2 phenotype⁸ which appears to be the dominate T cell phenotype in SSc^{3,6}.

IL-13 and IL-4 have been shown to augment collagen gel contraction in in vitro models using pulmonary fibroblasts, suggesting matrix remodelling⁹. Furthermore, overexpression of IL-13 in the lung in transgenic mice causes inflammation and lung fibrosis¹⁰, and an IL-13 inhibitor blocks the development of fibrosis in a Th2 dominant animal model in which animals are exposed to shistosomiasis¹¹. Disruption of the IL-4 gene in the Tight skin mouse (Tsk), a model of SSc in which the gene for fibrillin is mutated, reduces the fibrosis¹². However, the mechanism by which IL-13 cause's fibrosis is still to be elucidated.

MicroRNAs are small (around 21 nucleotides long) RNA molecules that function to regulate protein expression by translational inhibition or mRNA degradation through binding of the seed region with a complementary match site in the 3'UTR of the target mRNA¹³. It is now known that there are many miRs in the genome and that each miR can target hundreds of genes, thus the level of regulation of expression is huge. Emerging evidence suggest that miRs are involved in virtually all cellular processes including growth, differentiation, apoptosis and fibrosis¹⁴ and evidence has now been accrued that they are perturbed in multiple diseases. In SSc it has been found that there are

111 altered expression of various miRs and one of the most important is miR-29a which regulates
112 collagen directly through binding to its 3'UTR¹⁵ and enforced overexpression of miR-29a reduces
113 collagen levels in SSc dermal fibroblasts. MiR-29a has also been identified in fibrosis of the heart
114 after myocardial infarction¹⁶. Strategies that restore the levels of miR29a in vitro and in vivo reduce
115 fibrosis by targeting its mRNA target collagen1A1¹⁵. Thus modulation of miRs in vivo is a possible
116 therapeutic option in fibrosis. However, relatively few miRs have been described in SSc as compared
117 to other diseases such as cancer or diabetes for example. MiRS themselves can be regulated
118 epigenetically by methylation for instance and also histone modifications can also alter their
119 expression. Thus all the epigenetic modifications can each affect one another and underpins the
120 complexity of epigenetics. This study shows that miR-135b targets STAT6 and attenuates IL-13-
121 induced collagen expression.

122 **Results**

123 **IL-13 induces collagen independent of TGF- β signalling**

124 Because we had previously demonstrated that IL-13 derived from T cells induces collagen expression
125 in vitro we sought to confirm this in a 'cleaner' system free from other T cell cytokines
126 'contaminating' the system. To confirm that IL-13 induces collagen in isolated dermal fibroblasts we
127 performed a dose response study. Figure 1 demonstrates that 100 ng/ml of IL-13 induced the
128 highest fold change of collagen1A1 mRNA expression peaking at 3.5 fold change in expression
129 (normalised to 18S). This elevation of collagen was also found on the protein levels with a 72%
130 increase in collagen compared to control after IL-13 treatment (100 ng/ml). There was no change in
131 the expression of the myofibroblast marker α -smooth muscle actin expression by qRT-PCR at any
132 concentration of IL-13. It has also been suggested that IL-13 induces TGF- β 1 expression and release
133 and that TGF- β 1 is responsible for the collagen increase in a transgenic animal model of IL-13
134 overexpression causing lung fibrosis¹⁷. We did not observe any significant increase in TGF- β 1
135 expression after IL-13 stimulation by semi q-RT-PCR (figure 1B). Because TGF- β can also be activated
136 from in its latent form to a biologically active motif by the matricellular protein Thrombospondin-1
137 (TSP-1)^{18, 19} we measured the levels of TSP-1 in the conditioned media. ELISA of TSP-1 levels in
138 conditioned media after stimulation of dermal fibroblasts revealed no increase in secreted levels of
139 TSP-1 between control or IL-13 stimulation (mean value: 440 vs 428 pg/ml, $P = >0.05$ Student's t-
140 test). TGF- β 1 stimulation served as a positive control and was significantly different compared to
141 control and IL-13 treated (figure 1C). Direct measurement of TGF- β 1 also showed no significant
142 increase in expression (figure 1D). The target gene of TGF- β 1 CTGF was also measured by RT-PCR
143 and this was also not changed by the addition of exogenous recombinant IL-13 (data not shown). To
144 confirm the role of TGF- β in IL-13 mediated collagen1A1 induction cells were pre treated with the
145 TGF- β R inhibitor SB431542 and then stimulated with IL-13. Blockade of TGF- β signalling did not
146 significantly attenuate IL-13-mediated induction of collagen (figure 1E), thus indicating that TGF- β
147 signalling is independent of this effect. We further examined the expression of BMP and Activin
148 Membrane-Bound Inhibitor (BAMBI) which is part of the TGF family and is a negative regulator of
149 TGF- β 1 signalling and found that this was not different after IL-13 (1 fold control versus 0.89 IL-13
150 stimulated expression).

151 **IL-13 utilises STAT6 in collagen induction**

152 To examine the role of the transcription factor Signal Transducer and Activator of Transcription-6
153 (STAT-6) in IL-13 mediated collagen expression we used siRNA to deplete dermal fibroblasts of
154 STAT6. It was demonstrated that IL-13 addition (100 ng/ml) induced collagen1A1 expression, but this
155 was reduced by pre-treatment with specific siRNA against STAT6 significantly to 1.6 fold change

156 compared to control. Importantly, this was not reduced by the introduction of equivalent
157 concentration of scrambled control siRNA indicating its specificity (figure 2A) ($P= <0.05$ ANOVA).
158 Furthermore, chemical inhibition of STAT6 with the STAT6 specific inhibitor AS1517499²⁰ (40 nM)
159 lead also to a reduction of IL-13 mediated increases in collagen expression as compared to control
160 untreated cells (figure 2B). Figure 2C demonstrates the efficiency of the siRNAs against STAT6 by
161 measuring STAT6 transcripts with a 60% reduction in STAT6 transcripts after transfection of the
162 STAT6 siRNA and also protein expression (Student's t test) (figure 2D protein reduction).

163 **miR-135b regulates IL-13-mediated collagen expression**

164 We then used computational algorithm prediction software to identify possible miRs that target the
165 downstream signal molecule STAT6. These computer prediction software work on the basis of
166 putative seed pairing between the 'seed' region in the miR and the 3'UTR in its target mRNA thus
167 leading to target mRNA repression. These identified miR-135b as a miR likely to target STAT6 directly
168 through this seed region. Transfection of synthetic miR-135b mimics into dermal fibroblasts
169 attenuated the IL-13 induction of collagen1A1 expression; however the scrambled miR did not
170 attenuate the collagen induction by IL-13 stimulation (100 ng/ml) figure 3A (Significantly different
171 between control vs IL-13 treated and IL-13 treated plus miR135b mimic. No significant difference
172 between IL-13 treated vs IL-13 treated and scrambled miR mimic, ANOVA). To confirm that
173 transfection of miR-135b into the fibroblast was efficient in these cells we transfected a high and low
174 concentration and then measured the miR levels 24 hours later using qRT-PCR. Figure 3B
175 demonstrates the expression of miR-135b after transfection of low and high dose miR-135b. Figure
176 3C also demonstrates that transfection of miR-135b alone reduces STAT6 mRNA levels significantly.
177 However, it did not alter the levels of a similar STAT, STAT3 (figure 3D). Interestingly, miR-135b has a
178 binding site for the 3'UTR of Monocyte Chemoattraction Protein 3/CCL7 and should target this
179 directly we therefore measured MCP-3 after transfection of miR-135b. There was a reduction after
180 transfection of miR-135b of MCP-3 gene expression.

181 **Reduced levels of miR-135b in SSc fibroblasts and elevated STAT6**

182 The target of miR135b is STAT6 due to the prediction software analysis and also because of the
183 reduction of STAT6 with synthetic miRs we measured the levels in dermal fibroblasts in SSc patients
184 and found this to be elevated (figure 4A). Because we had found that miR-135b was regulating
185 STAT6 and mediating collagen expression we examined the levels of miR-135b in SSc dermal
186 fibroblasts. We found a reduced expression of miR-135b levels in SSc compared to control
187 fibroblasts, however, this did not quite reach statistical significance (figure 4B). Because TGF- β 1 is a
188 critical cytokine in fibrosis and is highly elevated in SSc we treated cells with TGF- β 1 (10 ng/ml) to
189 see if this reduced miR-135b. Unexpectedly, TGF- β 1 stimulation led to a 2 fold increase miR-135b
190 expression compared to untreated healthy control fibroblasts ($P =0.0354$ Student's t-test) (figure
191 4C), this was opposite to what we had hypothesised.

192 Dermal fibroblasts isolated from SSc patients were examined for IL-4R α expression as this is the
193 receptor subunit used by IL-13 (and IL-4) upstream of STAT6 and is common receptor through which
194 both cytokines signal. There was no clear difference in expression of the IL-4 receptor in SSc
195 fibroblasts (figure 4D). Because reactive oxidative species has been shown to play a prominent role
196 in fibrosis in SSc we incubated healthy control dermal fibroblast cells with sub toxic concentrations
197 H2O2 to examine its effect on IL-4R α expression. MTT assay demonstrated that the H2O2 treated
198 cells were not dying. qPCR demonstrated no significant difference in IL-4R expression between H2O2
199 treated and non-treated cells ($P=> 0.05$; Student's t test).

200 **Levels of serum and monocyte miR-135b**

201 It has recently been discovered that miRs can also be extracellular and that these miRs are enclosed
202 within vesicles called exosomes rendering them remarkably stable. Patient and healthy control
203 serum was isolated and measured for miR-135b by qRT-PCR and this demonstrated highly
204 significantly reduced levels of miR-135b compared to healthy controls ($P = 0.0060$ Student's t test)
205 (figure 5A). To elucidate this further we measured the levels of miR-135b in isolated CD14+
206 monocytes in patients and found this was significantly lower compared to controls (figure 5B).

207 **Bleomycin treated mice have lower miR-135b levels**

208 A useful model of skin fibrosis is the bleomycin model in which instillation of the compound
209 bleomycin into the mouse results in inflammation-driven fibrosis that recapitulates the fibrosis in
210 SSc. We measured the levels of miR-135b in the skin of mice treated with bleomycin or vehicle
211 control treated mice and found highly significantly reduced levels of miR-135b ($P = 0.0001$; Student's
212 t test) figure 5C). Pro- fibrotic TIMP-1 mRNA was also significantly elevated in the bleomycin mouse
213 tissue compared to vehicle control (figure 5D).

214 **Regulation of miR135b levels**

215 Because the miR appears to be regulating its target STAT6 and we had demonstrated STAT6 is
216 altering collagen levels and in SSc cells the miR was downregulated we wondered what is regulating
217 the repression of the miR itself? Examining the promoter sequence of the miR135b gene it could be
218 seen that it has CpG sites that could be methylated we therefore incubated healthy dermal
219 fibroblasts with the global demethylating agent 5'azaC which sequesters DNMT enzyme activity.
220 Incubation with 5'aza lead to significant upregulation of miR135b levels of 9 fold compared to
221 vehicle treated cells (figure 6A) ($P = <0.001$ Student's t test). However the same incubation of 5'azaC
222 did not lead to upregulation of the unrelated microRNA miR133a compared to vehicle control
223 treated cells (figure 6B). This indicates methylation is important in its regulation. In general
224 hypermethylation leads to gene repression and hypomethylation leads to enhanced gene
225 expression. Cytosine is the base that is methylated generating 5'methyl cytosine and it is now known
226 that TET enzymes are the enzymes responsible for removing this modification and appear important
227 in demethylation. We hypothesised that a reduction in the SSc dermal fibroblasts would be present
228 leading to altered demethylation. Figure 6C demonstrated no difference in TET1 levels suggesting
229 this is not a factor influencing this. We further examined the expression of the methyltransferase
230 enzyme Enhancer of Zeste Homologue 2 (Ezh2) which is important for the transfer of methyl groups
231 and this was reduced in the SSc fibroblasts but not statistically significant (figure 6D). There was also
232 no significant difference in the methyltransferase ASH1 (figure 6D). ASH1 is part of the trithorax
233 proteins and was recently shown to regulate fibrosis by binding directly to the TIMP-1 promoter.

234 Methyl cap binding protein 2 (MeCP2) is the protein most associated with the disease Rett syndrome
235 but is ubiquitously expressed²¹. This acts by binding to DNA to repress the DNA gene expression by
236 binding in its methyl binding domain. Because of its repressive function in DNA we examined its
237 expression. We found that MeCP2 is significantly enhanced in SSc dermal fibroblasts compared to
238 control fibroblastss (figure 6E). Furthermore in normal dermal fibroblasts exposure to TGF- β 1 leads to
239 significant elevation of MeCP2 expression, but does not appear to be dose dependant (figure 6F).

240 **Demethylation reduces collagen levels**

241 We have shown that miR135b is regulated by methylation and that this could be mediated by the
242 repressive protein MeCP2 so we examined the effects of 5'aza'c on collagen expression in

243 fibroblasts. Exposure to 5'aza'C reduced the levels of collagen1A1 compared to vehicle control
244 treated cells in healthy dermal fibroblasts (figure 7A). ($P= <0.001$ Student's t test).

245 Using SSc dermal fibroblasts we also found a significant reduction in collagen levels after 5'azaC
246 treatment also (figure 7B) (Student's t test $P= <0.05$). However, we could see no significant
247 difference in CTGF levels (figure 7C).

248

249

250

251 Discussion

252 Extracellular Matrix (ECM) production involves responses to endogenous and exogenous factors that
253 promote production of ECM or inhibit the breakdown of ECM. Excessive production leads to scarring
254 and fibrosis and is especially prominent in SSc. IL-13 is a pro fibrotic molecule that is produced by T
255 cells that activates ECM production and is a feature of many fibrotic diseases but its molecular
256 mechanism is not well described. IL-13 is elevated in SSc and is associated with disease specific
257 features such as nailfold capillary defects⁵ and IL-13 producing T cells are found within the skin.
258 Here we demonstrate that it is STAT6-dependant and that miR-135b regulates STAT6 by targeting
259 mRNA and that this miR may be reduced through a methylation dependant mechanism that may
260 include MeCP2.

261 IL-13 has been demonstrated to be elevated in the bleomycin model of fibrosis and activation of the
262 pregnane X receptor blocked the bleomycin induced fibrosis and this was not mediated directly but
263 through reducing the expulsion of IL-13 from murine T cells to activate the fibroblasts to secrete
264 ECM²², demonstrating the critical role of T cell mediated IL-13 in fibrosis. IL-13 has also been
265 described to suppress MMP-13 in isolated dermal fibroblasts thus decreasing the proteolytic
266 degradation of ECM favouring an increase in deposition²³ and also reduce MMP-3 release by ocular
267 conjunctiva fibroblasts and in lung fibroblasts IL-13 has been shown to induce Platelet Derived
268 Growth Factor (PDGF) release²⁴.

269 We have previously demonstrated that T cell-derived IL-13 can induce collagen transcription in
270 healthy dermal fibroblasts in culture⁶ and it is generally accepted that SSc has a Th2 dominance with
271 increased Th2 cytokines both locally and in the sera⁴ and these foster the release of ECM.
272 Furthermore, Fuschiotti et al using multi colour flow cytometry demonstrated that it is effector CD8+
273 T cells that are the highest producers of IL-13 in SSc, even though CD4+ T cells also display
274 production²⁵. They also found this CD8+ T cell production of IL-13 is associated with diffuse
275 cutaneous SSc more so than limited SSc²⁵. This has also been verified in a recent study with isolated
276 CD8+ T cells²⁶. It has also been shown that CD8+ T cells isolated from patients with SSc mediate
277 increased collagen1A and fibronectin expression in dermal fibroblasts in culture and that this can be
278 blocked by incubation with an anti-IL-13 antibody, but not by an anti-IL-4 antibody or isotype control
279 indicating this is IL-13 specific and not mediated through IL-4. The authors also show that incubation
280 of T cell supernatants with dermal fibroblasts promotes the phosphorylation of the transcription
281 factor STAT6 assessed by flow cytometry. We had also seen a similar effect⁶ in vitro. Indeed siRNA
282 mediated silencing of GATA3 in SSc CD8+ T cells from patients diminished high basal unstimulated
283 levels of IL-13. It has been published that IL-13-mediated increases in lung fibrosis by a transgene
284 expressing mouse was facilitated by TGF- β 1 and can be reduced by blocking the activation of TGF- β
285¹⁷, however we did not find any increase in TGF- β levels after IL-13 stimulation nor the TGF- β

286 activation protein TSP-1¹⁹. Furthermore blockade of the TGF- β R with chemical inhibition had no
287 effect on collagen induction by IL-13. We also found no change in BAMBI levels which is a negative
288 regulator of TGF- β signalling by acting as a pseudo receptor. This is in line with data in which IL-13
289 KO mice are protected from lung fibrosis but not IL-4 KO mice, despite the fact that they have
290 abundant TGF- β 1 levels. We demonstrate here that siRNA against STAT6 to silence the transcription
291 factor diminishes the collagen induction mediated by IL-13 stimulation and this was also the case
292 using the chemical STAT6 inhibitor that has previously been reported to inhibit STAT6 effects²⁰.
293 Thus, STAT6 is critical in mediating this response. However, it appears that TGF- β does not play a
294 role in this induction. IL-13 had been previously shown in lung fibroblasts to induce collagen through
295 TGF- β in fibroblasts from asthma patients²⁷. It has recently been demonstrated that methylation of
296 STAT6 determines its phosphorylation and modulates its DNA binding activity in response to
297 exogenous stimulation²⁸, thus adding another layer of complex regulation. Because IL-13 shares its
298 signalling with the shared co receptor IL-4 α we measured the levels of this, we could find no increase
299 in IL-4 α in SSc fibroblasts compared to controls and this could not be modulated by oxidative stress
300 either, as ROS is important in fibrogenesis.

301 Through computer prediction software we identified miR-135b as regulating STAT6 by binding to its
302 3'UTR region. We confirmed this with transfection of miR-135b and the reduction of STAT6 and
303 augmentation of IL-13 induction of collagen expression in these cells. Therefore, reduction of miR-
304 135b in SSc cells would lead to enhanced STAT6-mediated ECM induction. Interestingly we also
305 observed reduction of MCP-3 which is predicted to be targeted by miR-135b as it has a binding site.
306 This confirms transfection of the miR. MCP-3 is a chemoattractant for monocytes and monocytes are
307 important in the disease and are often found in the skin of SSc patients. A study has shown that
308 MCP-3 is elevated in SSc and the Tsk mouse model of fibrosis which has similar features to SSc. What
309 actually modulates the levels of miR-135b is unknown and maybe a variety of soluble factors,
310 possibly released by innate immune cells. We hypothesised that the pro fibrotic TGF- β 1 would
311 diminish miR-135b, however, it actually increased its expression. This may be part of a negative
312 feedback loop to dampen down fibrosis, however further investigations are required.

313 Using the bleomycin model which recapitulates features of the disease, we found also that miR135b
314 was significantly reduced in bleomycin treated mice. Many miRs have now been identified in
315 mediating a role in fibrosis, however only a very few have been described in SSc. We also show
316 reduced levels of miR135b in SSc dermal fibroblasts. It is known that miR-29a is involved in SSc¹⁵ and
317 we have also demonstrated reduced levels of miR-29a in SSc dermal fibroblasts²⁹ and this targets
318 collagen. Others have demonstrated down regulated miR let7-a in SSc by in situ hybridisation and
319 qRT-PCR and found that this contributes to excessive collagen production³⁰. Similarly in keloid
320 fibroblasts, which are abnormally excessive ECM type fibroblasts aberrant expression of miRs has
321 been demonstrated to mediate collagen1 expression³¹. The finding that miR-135b regulates collagen
322 expression via direct targeting of STAT6 further supports the notion that dysregulated miRs play a
323 role in fibrosis.

324 MiRs are very stable in serum and are released enclosed within membrane bound vesicles called
325 exosomes. These exosomes appear to protect the miR from endogenous RNAses that would
326 otherwise degrade the miR. We demonstrate for the first time reduced serum miR135b levels in SSc
327 patients compared to healthy controls. The significance of this is unknown but in further larger
328 studies if this is replicated this may be a potential biomarker. Because there were differences in
329 serum levels we sought to identify another cell type that might responsible for this, We found
330 significantly reduced levels in CD14+ monocytes in SSc patients. The significance of this is not clear

331 but one would expect its target STAT6 also to be elevated in the monocytes. STAT6 in monocytes is
332 important in M2 differentiation and these are important in wound healing.

333 We sought to identify what is underlying the repression of miR135b and because it was noted that it
334 has CpG sites that can be methylated in its promoter we hypothesised that the miR is
335 hypermethylated. We show through the use of the hypomethylating agent 5'aza'C that the miR was
336 elevated after treatment compared to vehicle control and furthermore an unrelated miR, miR133a
337 was not changed, suggesting that this is a specific event rather than a global one. Because it is now
338 known that TET1 enzyme is critical in the demethylation we examined the expression of this enzyme
339 in healthy and SSc fibroblasts and found no significant difference between the groups.

340 MeCP2 is a methylated binding protein that binds to methylated DNA to facilitate a repressive state
341 ²¹ and we hypothesised this may be modulated in SSc. We examined the levels of MeCP2 and found
342 this to be elevated in SSc fibroblasts. MeCP2 is part of a family of methyl CpG binding proteins and is
343 the most abundantly expressed member of this family ²¹. Mutations in the protein are more
344 commonly associated with Rett syndrome a rare X-linked neurodevelopmental disorder affecting 1
345 in 10000 females ³². Mutations are often found in the methyl binding domain of the protein and lead
346 to alterations in its levels in the brain, however, its precise molecular effects are unknown. We
347 demonstrate that elevated levels of MeCP2 may be associated with repression of miR135b and that
348 this could be forming a complex with HDAC1. We also found large upregulation of MeCP2 in healthy
349 cells upon TGF- β 1 stimulation. It is of note that a SNP in MeCP2 is associated with SSc ³³.
350 Furthermore, MeCP2 heterozygous mice have attenuated fibrosis in the liver after carbon
351 tetrachloride instillation with much lower myofibroblasts and collagen content ³⁴. Furthermore
352 MeCP2 has been found in fibrotic hearts ³⁵. This indicates that MeCP2 is critical in fibrosis.
353 Interestingly there also appears to be some interaction in liver fibrosis between MeCP2 and the
354 methyltransferase ASH1, where the increased expression of MeCP2 either through regulation of
355 miRs or another mechanism appears to elevate ASH1 levels and increases ECM through direct
356 binding of the genes in their promoters. Although we saw some elevation in SSc dermal fibroblasts
357 of ASH1 this was not statistically significant. It is suggested that the repression of miR135b is due to
358 methylation as there is methylation sites in the CpG islands in the miR135b promoter and due to the
359 fact that hypomethylation led to an increase in miR levels. Although 5'Aza'c is none specific in
360 demethylating it is suggested that it is demethylating the miR135b promoter and thus derepressing
361 this. This repression may be aided by MeCP2 that is binding the methylated DNA and helping to
362 repress it possibly in combination with HDAC1. In liver fibrosis this repression by MeCP2 and HDAC1
363 leads to repression of PPAR- γ and consequent silencing of this gene, PPAR γ itself is a negative
364 regulator of fibrosis and the reduction of this releases the ECM genes to be expressed ³⁴. Also a
365 transgenic mouse over expressing MeCP2 has exacerbated heart fibrosis and enhanced scarring in
366 response to pressure overload ³⁶.

367 Finally as well as the DNA demethylation increasing the levels of the miR it also demonstrated a
368 reduction in collagen expression.

369 In SSc dermal fibroblasts it has been shown that 5'Aza'C reduced hypermethylation of the Wnt
370 antagonist DKK1 and Secreted Frizzled RP1 (SFRP1) and thus enhanced their expression and this was
371 associated with a blockade of pro-fibrotic Wnt signalling and in vivo 5'Aza'C ameliorated bleomycin
372 induced fibrosis ³⁷. The blockade of fibrosis in the bleomycin model by hypomethylation could also
373 have been due in part to reactivation of repressed miR135b. The fact that SSc fibroblasts in culture
374 retain a fibrotic phenotype even over many passages suggests they have some sort of intrinsic
375 'memory', this could be due to the methylation that is imprinted and retained over multiple cell
376 divisions. It has been demonstrated in cardiac fibroblasts that hypoxia induced fibrosis is driven by a

377 global hypermethylation³⁸. This increased methylation is genome-wide and mediated by a hypoxia
378 inducible factor-dependant increase in DNMT3 as deletion in vitro of DNMT3 by siRNA reduced
379 methylation and also collagen and α -Sma content³⁸. This indicates the global alteration of
380 methylation is important in the differentiation of fibroblasts to myofibroblasts. The initial event that
381 is driving the methylation in their study is hypoxia and the heart is particularly vulnerable to a
382 hypoxic state. In our study we do not know what is increasing methylation but it is interesting to
383 note that hypoxia is prevalent in SSc and hypoxia has been shown to increase collagen expression in
384 dermal fibroblasts³⁹. It is suggested that hypoxia maybe leading to hypermethylation and increased
385 ECM by repression of miR135b. It is also interesting to note that mice exposed to hypoxia
386 experimentally have elevated ECM in their dermis³⁹.

387 Immune perturbations are common in SSc and precede the fibrosis. Here we demonstrate that the T
388 cell cytokine IL-13 mediates its effects through STAT6 and that STAT6-miR-135b are important in
389 collagen increases. Reintroduction of miR-135b may be useful in STAT6-driven fibrosis. We also
390 demonstrate the novel observation of elevated MeCP2 and that this may be important in SSc.

391 **Methods**

392 This study was approved by the local research ethics committee (REC no. 13/NE/0089
393 and 091/H0905/11) and all patients gave fully informed written consent. All methods were carried
394 out in accordance with the approved guidelines. Normal dermal fibroblasts were isolated from
395 healthy volunteers by skin punch biopsy (6 mm³) and from clinically diagnosed limited SSc patients
396 from the affected skin area and the tissue was placed into a six well plate with Dulbeccos modified
397 Eagles Medium (DMEM) medium (Sigma) supplemented with 10% (vol/vol) heat-inactivated Fetal
398 Calf Serum (FCS) (Gibco, UK) and 2 mM L-glutamine and 100U/ml penicillin/streptomycin at 37°C in
399 an atmosphere containing 5% CO₂. After a few days cells were confluent and passaged using
400 trypsin/EDTA (Gibco, UK) from the explant and all experiments were performed in early passaged
401 cells (p2-8). Control tissue was derived from healthy donors undergoing corrective abdominal
402 reduction (plastic) surgery N= 5. SSc patients were all female and not taking any immunosuppressive
403 therapy or chemotherapy and all had clinically diagnosed limited SSc n=5 mean age 57 years old (all
404 female SSc) taking no medication. The STAT6 inhibitor AS1517499²⁰ was purchased from
405 AxonMedchem (USA) and was used at a final concentration of 40 nM in cell culture experiments. The
406 TGF- β inhibitor SB431542 (Tocris Biosciences, UK) was used at a final concentration of 10 μ M to
407 inhibit the TGF- β signalling system. Fibroblasts were pre-treated for 2 hours with or without
408 SB431542 after which time IL-13 was incubated 100 ng/ml with the TGF- β inhibitor still within the
409 media, 24 hours later the cells were harvested.

410 **RT-PCR**

411 After cell stimulation cells were harvested in Trizol buffer and cellular RNA isolated according to the
412 manufacturer's instructions. RNA quality was assessed by nanodrop ND100 spectrophotometer with
413 260/280nm readings. 1 μ g RNA was reverse transcribed to cDNA with superscript III (Invitrogen, UK)
414 with RNase inhibitor. Prepared cDNA was subjected to quantitative PCR using SYBR green Taq ready
415 (Sigma, UK) technology using specific primers to the genes of interest using the specific primers
416 (forward and reverse) below in a total volume of 25 μ l using the 7500 RT-PCR machine (Applied
417 Biosciences, UK). Data was normalised to endogenous housekeeping gene 18S, which was confirmed
418 to be stable across the groups and relative changes were calculated using the deltadelta Ct method
419 with the control as the comparator. Collagen1A1: forward 5'-CAAGAGGAAGGCCAAGTCGAGG-3',
420 reverse 5'-CGTTGTCGACGACGAGAT-3' 18S Forward: 5' CGAATGGCTCATTAATCAGTTATGG-3'
421 Reverse 5'-TATTAGCTCTAGAATTAC CACAGTTATCC-3'. STAT6: Forward: 5'-CCTCGTCCACAGTTGCTT-3'

422 Reverse: 5'-TCCAGTGCTTTCTGCTCC-3'. STAT3: Forward: 5'-GGAGGAGTTGCAGCAAAAAG-3' Reverse:
423 5'-TGTGTTTGTGCCAGAATGT-3'
424 Absent, Small or Homeotic disc-1 (ASH1): Forward: 5'AATGATCTTTGCTGAGTGTT-3' Reverse:
425 TCCCAACCTTTTTCCTCAG-3'. Connective Tissue Growth Factor Forward: 5'-CTCGCGGCTTACCGACTG-
426 3' Reverse: 5'-GCACTTGAAGTCCACCGG-3' BMP And Activin Membrane-Bound Inhibitor (BAMBI):
427 Forward: 5'-CGCCACTCCAGCTACATCTT-3' Reverse: 5'-CAGATGTCTGTCGTGCTTGC-3'.
428 Alpha Smooth muscle actin: Forward: 5'-TGAAGAGCATCCACCT-3' Reverse: 50-
429 ACGAAGGAATAGCCACGC-3'. MCP-3/CCL7 Forward: 5'-TGTCTTTCTCAGAGTGGTTCT-3' Reverse: 5'-
430 TGCTTCCATAGGGACATCATA-3' IL-4R Forward: 5'-CTGGAGCACAACATGAAAAGG-3' Reverse: 5'-
431 AGTCAGTTGTCTGGACTCTG-3'. MeCP2: Forward: 5'- GATCAATCCCAGGGAAAAGC-3' Reverse: 5'-
432 CCTCTCCCAGTTACCGTGAAG-3'.

433 Semi quantitative PCR for TGF- β 1 was performed using primers for TGF- β 1 Forward: 5'-
434 GGATACCAACTATTGCTTCAGCTCC-3' Reverse: 5'-AGGCTCCAAATATAGGGGCAGGGTC-3' and the
435 product ran on a 2% agarose gel containing ethidium bromide and visualised under UV light.

436 **ELISA for Thrombospondin-1 (TSP-1) and TGF- β 1**

437 Healthy dermal fibroblasts were seeded into 24-well plates and at 80% confluence serum starved for
438 24 hours after which recombinant IL-13 100 ng/ml or 10 ng/ml Transforming Growth Factor- β (a
439 positive control) was added to serum free media and incubated for a further 24 hours. Conditioned
440 medium was then collected and measured for TSP-1 using a human TSP-1 ELISA (R&D systems, UK) in
441 accordance with the manufacturer's instructions against a standard curve of recombinant TSP-1
442 using a fluorescent plate reader (Tecan). The same supernatants were used to measure TGF- β 1
443 levels by ELISA (R&D systems, UK).

444 **siRNA knockdown**

445 For the siRNA silencing experiments cells were seeded into 24-well plates, and at 50–60% confluence
446 100 nM STAT6 siRNA SMARTpool (Dharmacon, UK) 100 nM of none targeting control siRNA was
447 transfected using DharmaFECT 1 in antibiotic and serum-free DMEM media. Following 24 h of
448 incubation, medium was replaced with fresh medium FCS free medium supplemented with
449 recombinant endotoxin-free IL-13 100 ng/ml (R&D systems, Abingdon, UK) and after a further 24 h
450 cells were harvested for expression.

451 **Western Blotting**

452 After transfection with specific siRNA or none targeting control siRNA (100 nM) cells were lysed in
453 RIPA buffer containing protease inhibitors. 25 μ g of total protein was loaded in Lammeli buffer with
454 beta-mecaptoethanol and ran on a 10% Polyacrylamide denaturing gel. The gel was transferred to
455 onto nitrocellulose membrane with wet transfer, blocked for 1 hour in 5% blocking solution (non-fat
456 milk) in TBS-tween and then hybridised overnight with anti-STAT6 antibody (Cell signal, 9362)
457 overnight 1:800 at 4°C, washed three times in TBS-tween and then incubated with anti-Rabbit Horse
458 Radish Peroxidase (HRP) antibody 1:4000 (Dako, UK) for 1 hour at room temperature, washed and
459 then incubated with ECL substrate (Biorad, UK) and then exposed and developed. Healthy or SSc
460 dermal fibroblast early passage were seeded and then lysed and then probed with anti-STAT6 1:800
461 or Ten Eleven Translocation-1 (TET1) (Abcam, UK) 1:700 or GAPDH (Abcam, UK) 1:8000. In some
462 experiments healthy dermal fibroblasts were treated with increasing doses of recombinant TGF- β 1
463 and then lysed and then probed for MeCP2 using an MeCP2 specific antibody (Ab2828) and the
464 re probed for β -actin (Ab8226).

465 **miR Experiments**

466 miR-135b was identified by prediction software to bind the 3'UTR of STAT6 (Pictar software and
467 Targetscan). Pre miR-135b (Thermo scientific, UK) was transfected into dermal fibroblasts at 75nM
468 concentration using dharmafECT1 transfection reagent in antibiotic and FCS-free medium along with
469 control miR (75nM). The sequence of the control miR is designed to be complementary to the
470 nematode worm *C. elegans*. To confirm successful transfection the miR was measured in the cells
471 after transfection after three washes with sterile PBS (Sigma, UK) using qRT-PCR with specific
472 primers for miR-135b (Applied Biosciences).

473 **H202 treatment**

474 Healthy dermal fibroblasts were grown to confluence and then treated with H202 (Sigma, UK) at sub
475 toxic concentrations 200µM for 2 hours in FCS-free medium after 2 hours the H202 FCS-free medium
476 was removed and replaced with complete medium containing 10% FCS and L-glutamine. These cells
477 were left for 3 days after which RNA was isolated and cDNA generated and qPCR was performed for
478 IL-4Rα with the primers described in the section above.

479 **Measurement of miR-135b**

480 MiR-135b was measured in SSc dermal fibroblasts and healthy control cells using qRT-PCR and
481 normalised to let-7a levels using Taqman qPCR with primer specific reverse transcription. miR133a
482 was also measured after 5aza'c treatment also. Serum levels of miR-135 was measured by qRT-PCR
483 and also let7a after isolation with the miRNeasy RNA isolation kit (Qiagen, UK) following the
484 manufacturer's instructions. This serum miR study included larger number of patients as opposed to
485 the dermal fibroblasts study. The number of patients was 15, n=10 diffuse SSc and limited SSc
486 patients n=5. In some experiments healthy control dermal fibroblasts were treated with TGF-β1 (10
487 ng/ml) and after 24hrs RNA was harvested and qRT-PCR was performed for miR-135b and let7a as
488 the endogenous internal control. In further experiments CD14+ monocytes were isolated from
489 whole blood by negative selection and then RNA was isolated and miR-135b was measured along
490 with let-7a.

491 **Collagen measurement**

492 Total soluble collagen in cell culture supernatants was quantified using the SirCol collagen assay
493 (Biocolor, Belfast, UK) as per the manufacturer's instructions. Which is an assay based on
494 hydroxyproline. The dermal fibroblast were treated with nothing or IL-13 (100 ng/ml) and after 24
495 hours the collagen protein was quantitated. Data was normalized to control which was set at 100%
496 collagen.

497 **5'aza'2-deoxycytidine(5'aza'C) treatment**

498 Human dermal fibroblasts were treated with 10 µM of 5'aza'C (Sigma, UK) or vehicle control DMSO
499 for up to 5 days after which the miRs were measured as above. In separate experiments healthy and
500 SSc fibroblasts were treated with 10µM 5'aza'C or vehicle for 5 days and qPCR was performed for
501 collagen, CTGF and 18S.

502 **Bleomycin induced fibrosis**

503 Wild type C57BL/6 mice were used in this study. All the mice were male and aged 8-10 weeks old
504 at commencement of the study. Mice were anaesthetised with isoflurane, their backs shaved and 100
505 µl 0.5 mg/ml bleomycin (Apollo Scientific, UK) or saline (vehicle control) administered via
506 subcutaneous injection to an area approximately 1 cm². Injections were repeated every other day
507 for 4 weeks at which point mice were sacrificed (5 mice per group; treatment or vehicle).

508 **Wax embedded sample processing for miR quantification**

509 Skin biopsies were taken from the vehicle treated and bleomycin treated mice placed in 10%
510 formaldehyde for 16 hours after which time they were dehydrated through graded ethanols and
511 then placed in zylene, samples were then embedded into wax and then sectioned. 10µm sections
512 were then used to isolate RNA using the miRNeasy FFPE kit (Qiagen, UK) which includes removing
513 from the paraffin wax and treating with proteinase K digestion and isolation according to the
514 manufacturer's protocol. Tissue isolated RNA was measured for quality and reverse transcribed for
515 miR135b and let7a (Applied Biosystems; Id 4427975) using qRT-PCR with taqman™ probes. Data is
516 normalised to let7a and shown as fold change compared to vehicle treated mice. Sections were also
517 taken for the analysis of TIMP-1 by qPCR and normalised to 18s as the internal housekeeper. Mouse
518 TIMP-1 Primers: Forward: 5'-CAGTAAGGCCTGTAGCTGTGC-3' and 5'-CTCGTTGATTCGGGGAAC-3'.

519 **Statistical analysis**

520 Statistical analysis was performed between groups with a Student's T test or Analysis of Variance
521 (ANOVA) with *P* values <0.05 considered statistically significant * indicates significance in graphs.

522

523

524 **Figure legends**

525 **Figure 1 Dose response relationship of IL-13 and collagen induction. (A)** Dermal fibroblasts were
526 incubated with increasing doses of IL-13 in vitro and collagen1A1 was measured by qRT-PCR. Data
527 shown is the fold change normalised to 18S housekeeping mRNA data is mean and standard
528 deviation n=4. **(B)** Representative semi-quantitative RT-PCR of TGF- β 1 after stimulation of cells
529 with IL-13 for 24 hours PCR cycling was performed for 25 cycles and amplicons were
530 electrophoresed on a 2% agarose gel with ethidium bromide incorporated within and imaged
531 under UV light. 18S was used as an internal control NT: No template control, A untreated, B: IL-13
532 (100 ng/ml) 24 hours treatment. **(C)** Fibroblast conditioned medium was analysed by ELISA for
533 TSP-1 after removal of FCS and stimulation with IL-13 (100 ng/ml). TGF- β 1 stimulation served as a
534 positive control, data are the mean and SD from 4 independent experiments. **(D)** Fibroblast
535 conditioned media was measured for TGF- β 1 after stimulation with IL-13 **(E)** Dermal fibroblasts
536 were treated with the TGF- β R blocker SB431542 or untreated and then stimulated with IL-13 (100
537 ng/ml) and after 24 hours collagen1A1 mRNA was quantified by qRT-PCR and normalised to 18S.
538 Data is the mean and SD n=4.

539 **Figure 2 IL-13 mediates collagen production via STAT6 signalling. (A)** Dermal fibroblasts were
540 transfected with smartpool siRNA against STAT6 or none targeting siRNA at equal concentrations
541 after 24 hours medium was replaced with serum free medium containing IL-13 (100 ng/ml) after a
542 further 24 hours in culture qRT-PCR was performed for collagen1A1. **(B)** Dermal fibroblasts were
543 incubated with IL-13 (100 ng/ml), the STAT6 inhibitor (40 nM) and IL-13 or AS1517499 alone after
544 24 hours qRT-PCR was performed for collagen1A1. Data is the mean and SD and is normalised to
545 18S and untreated was set to 1 n=5. **(C)** Significant reduction in STAT6 after transfection with
546 specific STAT6 siRNA. Data is fold change compared to scrambled none specific siRNA after
547 transfection using DharmaFECT1 transfection. Data are the mean and SD n= 4 significant
548 difference Students t test. **(D)**. Representative western blot of STAT6 after scrambled control
549 siRNA transfection or specific STAT6 siRNA after transfection using DharmaFECT1 n=4.

550 **Figure 3 miR-135b targets STAT6 to reduce collagen induction. (A)** Dermal fibroblasts were
551 transfected with miR135b mimics or concentration matched control miR (*C. elegans*) for 24 hours
552 after which time the medium was replenished and contained 100 ng/ml recombinant IL-13 for a
553 further 24 hours after which time the cells were harvested and qPCR was performed for
554 collagen1A1 and normalised to 18s. Data is the mean and SD n=5 five different donors. **(B)** 75 nM
555 of 135b mimic (low dose) or 150 nM (high dose) was transfected into dermal fibroblasts and after
556 24 hours post transfection miR135b was quantitated by qRT-PCR, data is the mean and standard
557 deviation. **(C)**. 75nM of 135b mimic was transfected into dermal fibroblast and after 24 hours post
558 transfection STAT6 was quantified by qRT-PCR, data is normalised to 18S and compared to
559 scrambled miR transfected n=5 from five different individual donors. **(D)** STAT3 levels were
560 analysed by qPCR after transfection with miR135b mimic or control miR 24 hours post
561 transfection. Data is the mean and SD. ns: no significant difference between groups.

562 **Figure 4 Elevated miR135b target STAT6 SSc fibroblasts. (A)** Dermal fibroblasts or SSc fibroblasts
563 were isolated and cultured within the first three passages the cells were lysed and a western blot
564 was performed for STAT6. Representative western blot from 2 individual donors. GAPDH was used
565 as the loading control for equal loading **B)** Healthy and SSc fibroblasts the RNA was harvested and
566 qRT-PCR was performed for the expression of miR-135b and normalised to the expression of let7a.
567 Data is the mean and SD n=3. No significant difference. **(C)** Down regulation of miR-135b by TGF-
568 β 1. Dermal fibroblasts were stimulated with TGF- β 1 (10 ng/ml) and after 24 hours the RNA was
569 harvested and qRT-PCR was performed for miR-135b and normalised to the expression of let7a.

570 Data is the mean and SD n= 8. Significantly different compared to control (Student's t test). D). SSc
571 dermal fibroblasts express IL-4R α chain. Fibroblasts were isolated and cultured and then RNA
572 harvested then qRT-PCR was performed for IL-4R α and normalised to 18S. Data is the mean and
573 SD n=3. ns: no-significant difference between groups.

574 Figure 5 SSc sera has reduced miR-135b levels. (A) SSc and healthy control serum was measured
575 for miR-135b and let7a by qRT-PCR. Data is the mean and SD of HC=12 and SSc =15 ($P=0.006$
576 Student's t-test). (B) CD14⁺ cells were isolated and levels of miR-135b and let7a were measured by
577 qRT-PCR. Data is the mean and SD n= 7 ($P=0.03$ Student's t-test). (C) Bleomycin treated fibrotic mice
578 have diminished miR-135b levels. C56/B Mice were vehicle or bleomycin treated and after fibrosis
579 established skin biopsies were taken and the levels of miR135b were measured by RT qPCR and
580 the data was normalised to let7a. Data is the mean and SD of five animals per group n= 5 ($P=$
581 0.0001 Student's t test). (D) TIMP-1 levels were analysed by qPCR. Data is the mean and SD of five
582 animals per group n=5 ($P= 0.0001$ Student's t test).

583 Figure 6 Methylation regulates miR135b. A). Healthy dermal fibroblasts were treated with vehicle
584 control (DMSO) or 10 μ M 5'Aza'c for 5 days in culture after which qPCR was performed for miR135
585 and let7a data is normalised to let7a and compared to vehicle control data is the mean and SD of 5
586 individual donors n=5 (B) MiR133a levels were measured by qPCR and normalised to let7a. Data is
587 the mean and SD of five individual donors n=5 C). Healthy and SSc dermal fibroblasts express
588 similar levels of the DNA modifying enzyme TET1. Representative western blot for TET1 from two
589 individual donors with limited SSc. GAPDH is used as the loading control n= 4. (D). Healthy or SSc
590 dermal fibroblasts were analysed by qPCR for the genes Ezh2 and ASH1 and data normalised to
591 18s. The data is the mean and SD n= 4 ns: no significant difference between groups E). SSc
592 fibroblasts express higher MeCP2 levels. Healthy or SSc dermal fibroblasts were analysed by qPCR
593 for MeCP2 expression and the data normalised to 18S. The data is the mean and SD n=4 ($P=<0.001$
594 Student's t test). (F). Western blot of fibroblasts treated with increasing doses of TGF- β 1 for
595 MeCP2 levels. B actin served as a loading control.

596 Figure 7 Treatment with the global hypomethylating compound 5'Aza'c reduced collagen levels.
597 A). Healthy dermal fibroblasts were treated with DMSO vehicle control or 5'Aza'c for four days
598 after which qPCR was performed for collagen1A1 and 18S. Data is the mean and SD of five donors
599 and was normalised to 18S n=5. B). SSc dermal fibroblasts were treated with DMSO vehicle control
600 or 5'Aza'c for four days after which qPCR was performed for collagen and 18S. Data is the mean
601 and SD normalised to 18S n=4 C). SSc dermal fibroblasts were treated with DMSO control or
602 5'Aza'c for four days after which CTGF and 18S was measured by qPCR. Data is the mean and SD
603 n=4 ns: no significant difference between groups (Student's t test).

604 Acknowledgments

605 This work was supported by a2015/16/S/NZ6/00041 grant from the national Science Center
606 (Poland).

607 Author Contributions

608 SOR performed experiments and wrote the manuscript. MC performed some experiments and
609 helped draft the manuscript. NF and SP performed some experiments. JvL drafted and commented
610 on the manuscript and had oversight of the project.

611 Competing financial interests

612 The authors declare no competing financial interests.

613

614

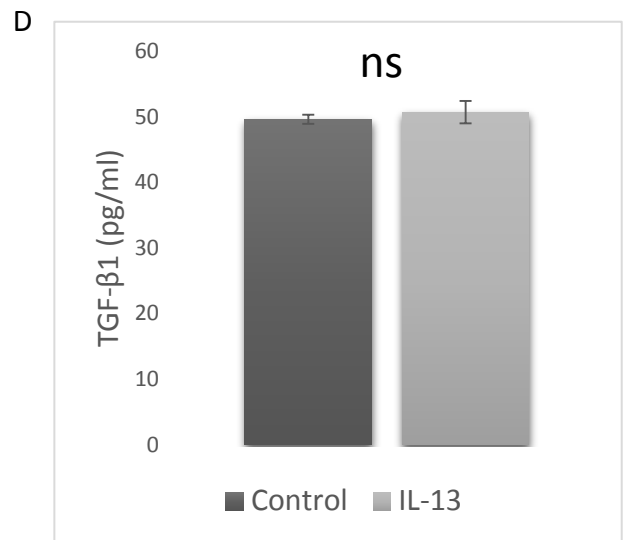
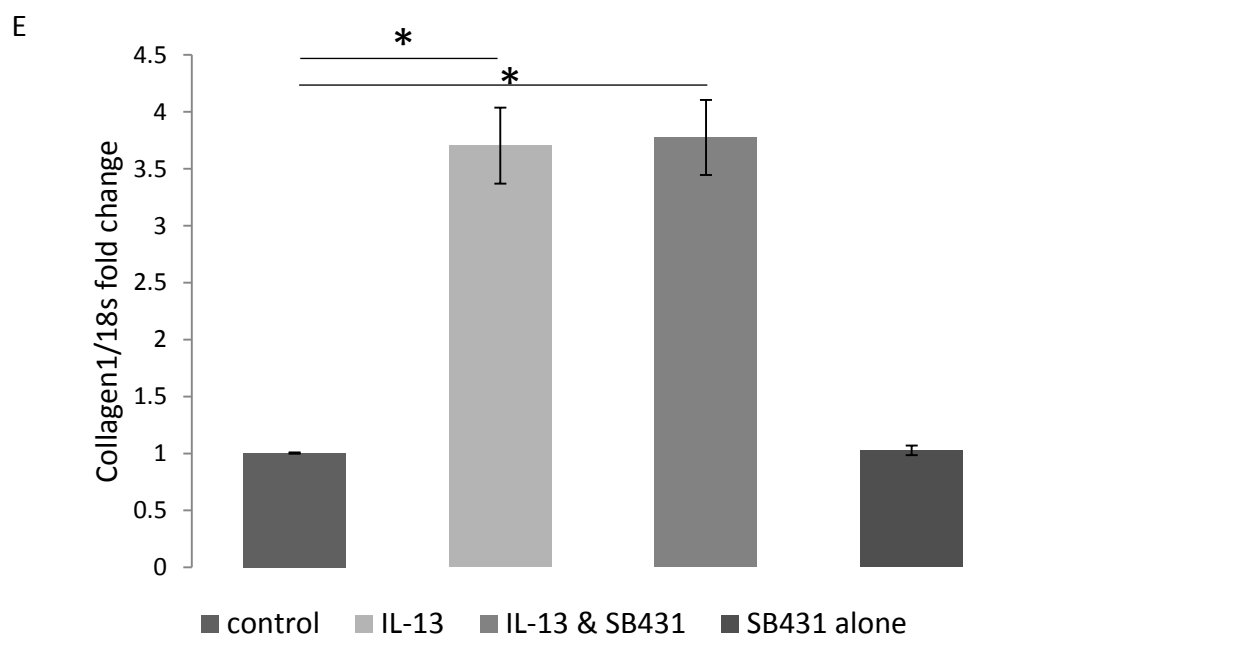
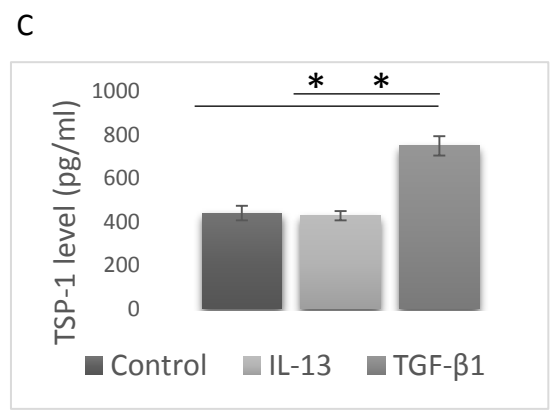
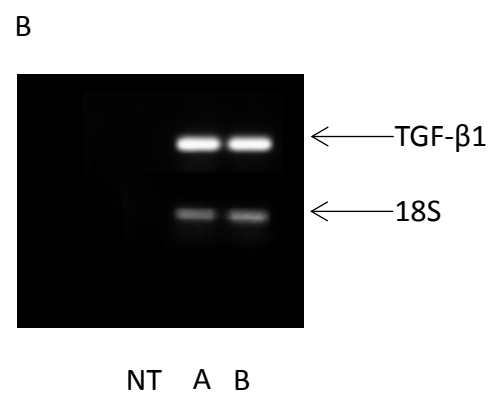
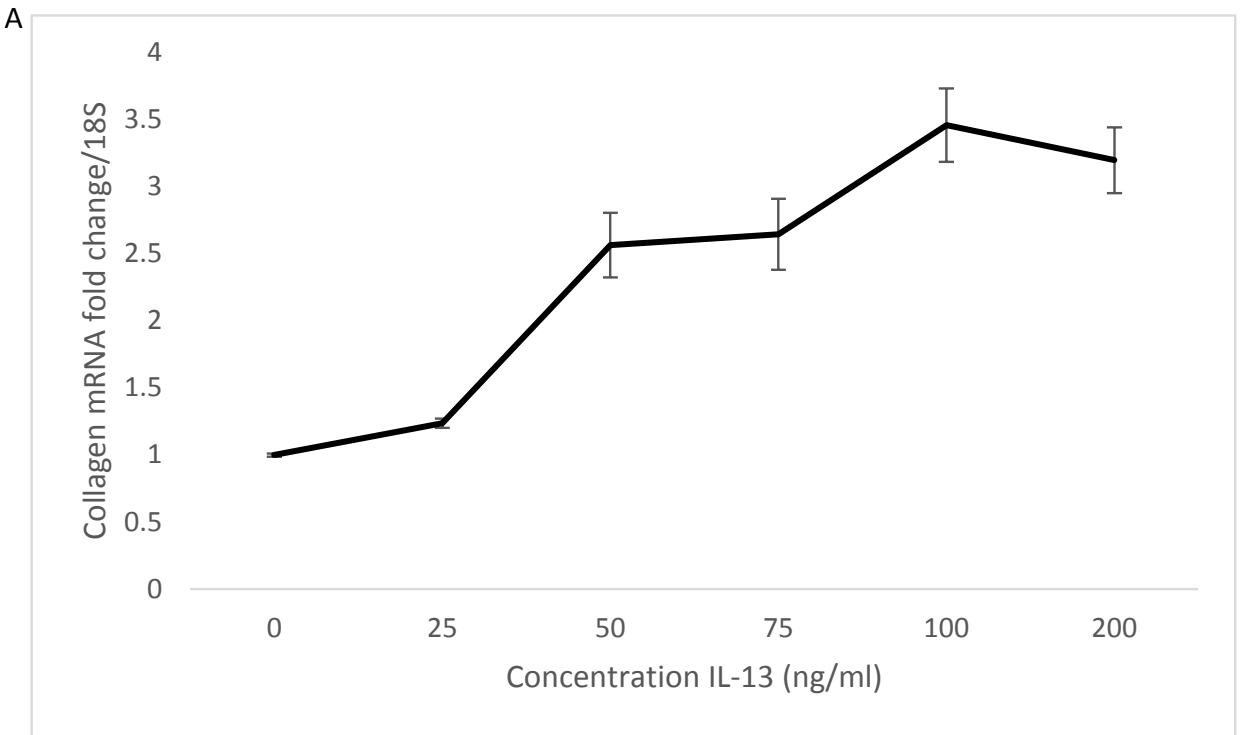
615 **References**

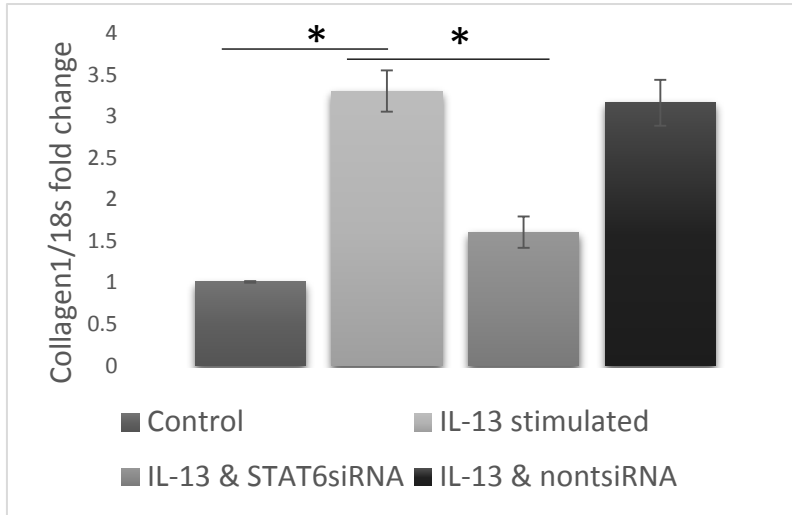
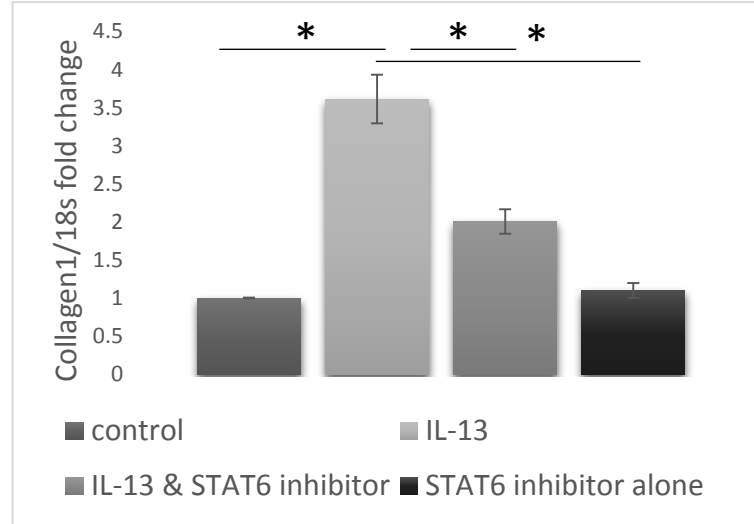
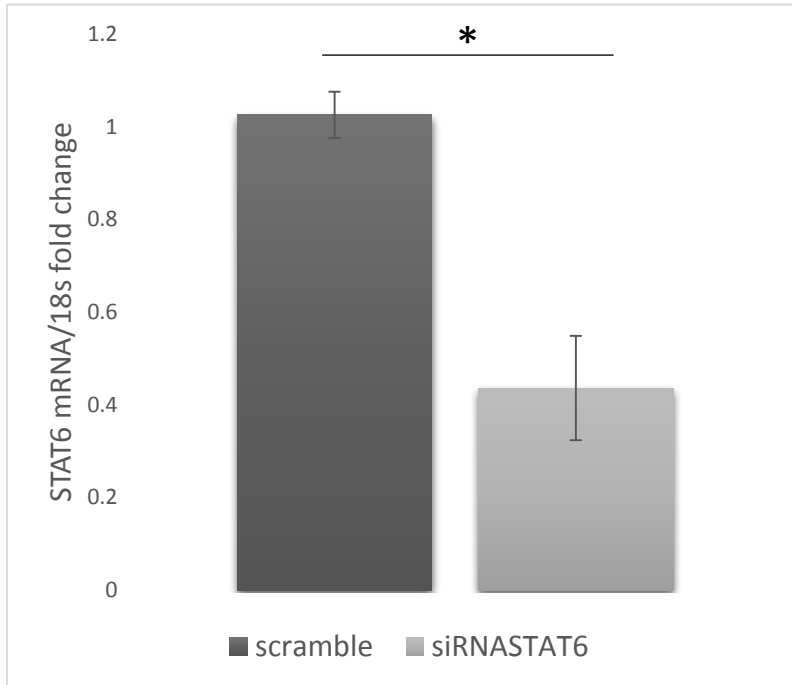
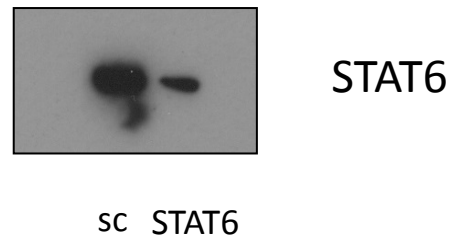
- 616 1. Gabrielli, A., Avvedimento, E.V. & Krieg, T. Scleroderma. *New England Journal of Medicine*
617 **360**, 1989-2003 (2009).
- 618 2. Kalogerou, A. et al. Early T cell activation in the skin from patients with systemic sclerosis.
619 *Annals of the Rheumatic Diseases* **64**, 1233-1235 (2005).
- 620 3. Hasegawa, M., Fujimoto, M., Kikuchi, K. & Takehara, K. Elevated serum levels of interleukin 4
621 (IL-4), IL-10, and IL-13 in patients with systemic sclerosis. *Journal of Rheumatology* **24**, 328-
622 332 (1997).
- 623 4. Atamas, S.P. et al. Production of type 2 cytokines by CD8+ lung cells is associated with
624 greater decline in pulmonary function in patients with systemic sclerosis. *Arthritis &*
625 *Rheumatism* **42**, 1168-1178 (1999).
- 626 5. Riccieri, V. et al. Interleukin-13 in systemic sclerosis: relationship to nailfold capillaroscopy
627 abnormalities. *Clin Rheumatol* **22**, 102-106 (2003).
- 628 6. Hügler, T. et al. Tumor necrosis factor–costimulated T lymphocytes from patients with
629 systemic sclerosis trigger collagen production in fibroblasts. *Arthritis & Rheumatism* **65**, 481-
630 491 (2013).
- 631 7. Kaplan, M.H., Schindler, U., Smiley, S.T. & Grusby, M.J. Stat6 Is Required for Mediating
632 Responses to IL-4 and for the Development of Th2 Cells. *Immunity* **4**, 313-319 (1996).
- 633 8. Zheng, W.-p. & Flavell, R.A. The Transcription Factor GATA-3 Is Necessary and Sufficient for
634 Th2 Cytokine Gene Expression in CD4 T Cells. *Cell* **89**, 587-596 (1997).
- 635 9. Liu, X. et al. Th2 cytokine regulation of type I collagen gel contraction mediated by human
636 lung mesenchymal cells *American Journal of Lung Cellular and Molecular Physiology* **282**,
637 1049-1056 (2002).
- 638 10. Zhu, Z. et al. Pulmonary expression of interleukin-13 causes inflammation, mucus
639 hypersecretion, subepithelial fibrosis, physiologic abnormalities, and eotaxin production.
640 *The Journal of Clinical Investigation* **103**, 779-788 (1999).
- 641 11. Chiaramonte, M. et al. An IL-13 inhibitor blocks the development of hepatic fibrosis during a
642 T-helper type 2–dominated inflammatory response. *The Journal of Clinical Investigation* **104**,
643 777-785 (1999).
- 644 12. Koderá, T., McGaha, T.L., Phelps, R., Paul, W.E. & Bona, C.A. Disrupting the IL-4 gene rescues
645 mice homozygous for the tight-skin mutation from embryonic death and diminishes TGF- β
646 production by fibroblasts. *Proceedings of the National Academy of Sciences* **99**, 3800-3805
647 (2002).
- 648 13. Bartel, D.P. MicroRNAs: Target Recognition and Regulatory Functions. *Cell* **136**, 215-233
649 (2009).
- 650 14. Chen, C.-Z., Li, L., Lodish, H.F. & Bartel, D.P. MicroRNAs Modulate Hematopoietic Lineage
651 Differentiation. *Science* **303**, 83-86 (2004).
- 652 15. Maurer, B. et al. MicroRNA-29, a key regulator of collagen expression in systemic sclerosis.
653 *Arthritis & Rheumatism* **62**, 1733-1743 (2010).
- 654 16. van Rooij, E. et al. Dysregulation of microRNAs after myocardial infarction reveals a role of
655 miR-29 in cardiac fibrosis. *Proceedings of the National Academy of Sciences* **105**, 13027-
656 13032 (2008).
- 657 17. Lee, C.G. et al. Interleukin-13 Induces Tissue Fibrosis by Selectively Stimulating and
658 Activating Transforming Growth Factor β 1. *The Journal of Experimental Medicine* **194**, 809-
659 822 (2001).
- 660 18. Ribeiro, S.M.F., Poczatek, M., Schultz-Cherry, S., Villain, M. & Murphy-Ullrich, J.E. The
661 Activation Sequence of Thrombospondin-1 Interacts with the Latency-associated Peptide to
662 Regulate Activation of Latent Transforming Growth Factor- β . *Journal of Biological Chemistry*
663 **274**, 13586-13593 (1999).

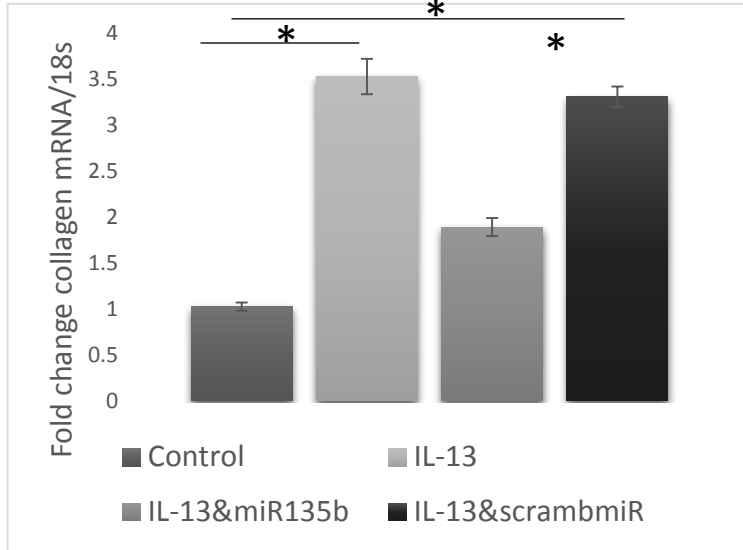
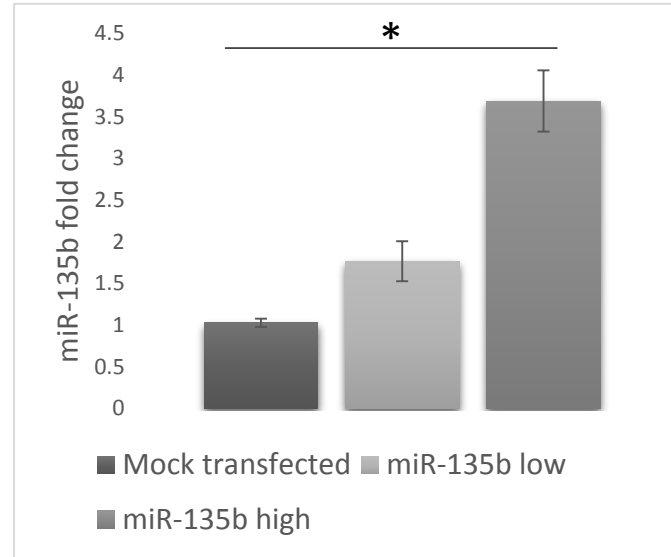
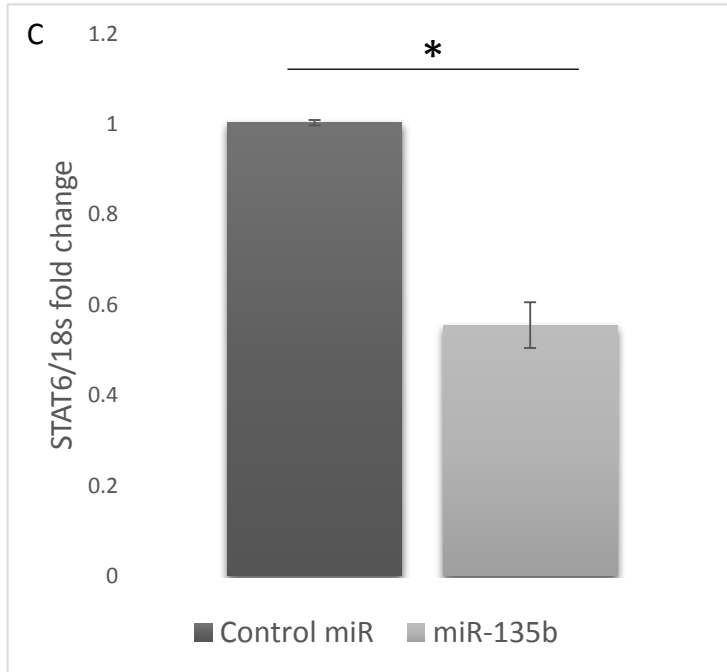
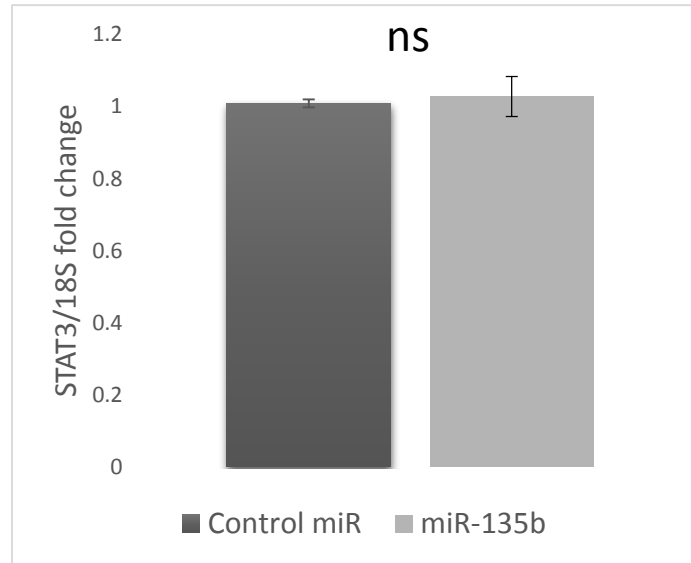
- 664 19. Sakai, K. et al. Thrombospondin-1 promotes fibroblast-mediated collagen gel contraction
665 caused by activation of latent transforming growth factor β -1. *Journal of Dermatological*
666 *Science* **31**, 99-109 (2003).
- 667 20. Chiba, Y., Todoroki, M., Nishida, Y., Tanabe, M. & Misawa, M. A Novel STAT6 Inhibitor
668 AS1517499 Ameliorates Antigen-Induced Bronchial Hypercontractility in Mice. *American*
669 *Journal of Respiratory Cell and Molecular Biology* **41**, 516-524 (2009).
- 670 21. Tudor, M., Akbarian, S., Chen, R.Z. & Jaenisch, R. Transcriptional profiling of a mouse model
671 for Rett syndrome reveals subtle transcriptional changes in the brain. *Proceedings of the*
672 *National Academy of Sciences* **99**, 15536-15541 (2002).
- 673 22. Beyer, C. et al. Activation of pregnane X receptor inhibits experimental dermal fibrosis.
674 *Annals of the Rheumatic Diseases* **72**, 621-625 (2013).
- 675 23. Moriya, C. et al. Expression of Matrix Metalloproteinase-13 Is Controlled by IL-13 via
676 PI3K/Akt3 and PKC-[delta] in Normal Human Dermal Fibroblasts. *J Invest Dermatol* **131**, 655-
677 661 (2011).
- 678 24. Ingram, J.L. et al. Opposing Actions of Stat1 and Stat6 on IL-13-Induced Up-Regulation of
679 Early Growth Response-1 and Platelet-Derived Growth Factor Ligands in Pulmonary
680 Fibroblasts. *The Journal of Immunology* **177**, 4141-4148 (2006).
- 681 25. Fuschiotti, P., Medsger, T.A. & Morel, P.A. Effector CD8+ T cells in systemic sclerosis patients
682 produce abnormally high levels of interleukin-13 associated with increased skin fibrosis.
683 *Arthritis & Rheumatism* **60**, 1119-1128 (2009).
- 684 26. Ayano, M. et al. Increased CD226 Expression on CD8+ T Cells Is Associated with Upregulated
685 Cytokine Production and Endothelial Cell Injury in Patients with Systemic Sclerosis. *The*
686 *Journal of Immunology* **195**, 892-900 (2015).
- 687 27. Firszt, R. et al. Interleukin-13 induces collagen type-1 expression through matrix
688 metalloproteinase-2 and transforming growth factor- β 1 in airway fibroblasts in asthma.
689 *European Respiratory Journal* **43**, 464-473 (2014).
- 690 28. Chen, W., Daines, M.O. & Hershey, G.K.K. Methylation of STAT6 Modulates STAT6
691 Phosphorylation, Nuclear Translocation, and DNA-Binding Activity. *The Journal of*
692 *Immunology* **172**, 6744-6750 (2004).
- 693 29. Ciechomska, M., van Laar, J.M. & O'Reilly, S. Emerging role of epigenetics in systemic
694 sclerosis pathogenesis. *Genes Immunity* **15**, 433-439 (2014).
- 695 30. Makino, K. et al. The Downregulation of microRNA let-7a Contributes to the Excessive
696 Expression of Type I Collagen in Systemic and Localized Scleroderma. *The Journal of*
697 *Immunology* **190**, 3905-3915 (2013).
- 698 31. Kashiya, K. et al. miR-196a Downregulation Increases the Expression of Type I and III
699 Collagens in Keloid Fibroblasts. *J Invest Dermatol* **132**, 1597-1604 (2012).
- 700 32. Amir, R.E. et al. Rett syndrome is caused by mutations in X-linked MECP2, encoding methyl-
701 CpG-binding protein 2. *Nat Genet* **23**, 185-188 (1999).
- 702 33. Carmona, F.D. et al. New insight on the Xq28 association with systemic sclerosis. *Annals of*
703 *the Rheumatic Diseases* **72**, 2032-2038 (2013).
- 704 34. Mann, J. et al. MeCP2 Controls an Epigenetic Pathway That Promotes Myofibroblast
705 Transdifferentiation and Fibrosis. *Gastroenterology* **138**, 705-714.e4 (2010).
- 706 35. Feng, Y., Huang, W., Wani, M., Yu, X. & Ashraf, M. Ischemic Preconditioning Potentiates the
707 Protective Effect of Stem Cells through Secretion of Exosomes by Targeting Mecp2 via miR-
708 22. *PLoS ONE* **9**, e88685 (2014).
- 709 36. Mayer, S.C. et al. Adrenergic Repression of the Epigenetic Reader MeCP2 Facilitates Cardiac
710 Adaptation in Chronic Heart Failure. *Circulation Research* **117**, 622-633 (2015).
- 711 37. Dees, C. et al. The Wnt antagonists DKK1 and SFRP1 are downregulated by promoter
712 hypermethylation in systemic sclerosis. *Annals of the Rheumatic Diseases* **73**, 1232-1239
713 (2014).

- 714 38. Watson, C.J. et al. Hypoxia-induced epigenetic modifications are associated with cardiac
715 tissue fibrosis and the development of a myofibroblast-like phenotype. *Human Molecular*
716 *Genetics* **23**, 2176-2188 (2014).
- 717 39. Distler, J.H.W. et al. Hypoxia-induced increase in the production of extracellular matrix
718 proteins in systemic sclerosis. *Arthritis & Rheumatism* **56**, 4203-4215 (2007).

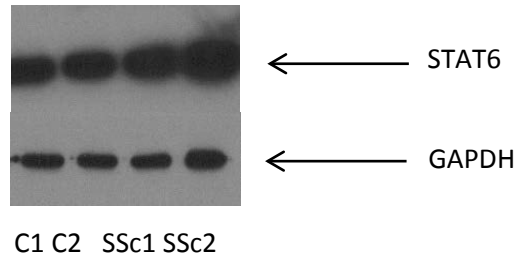
719



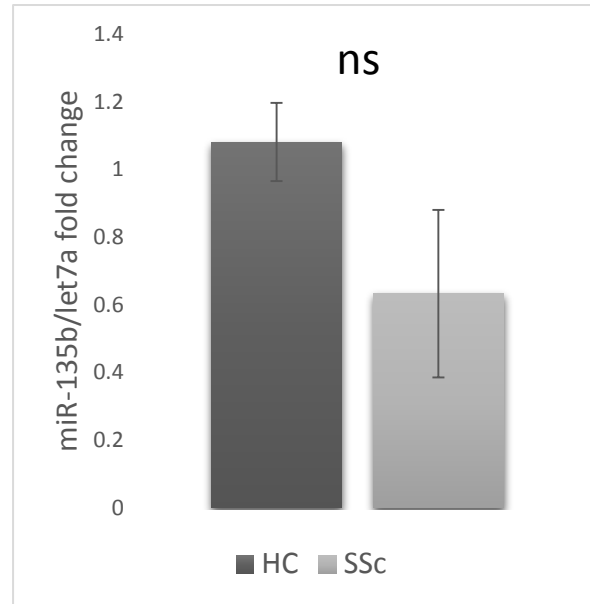
A**B****C****D**

A**B****C****D**

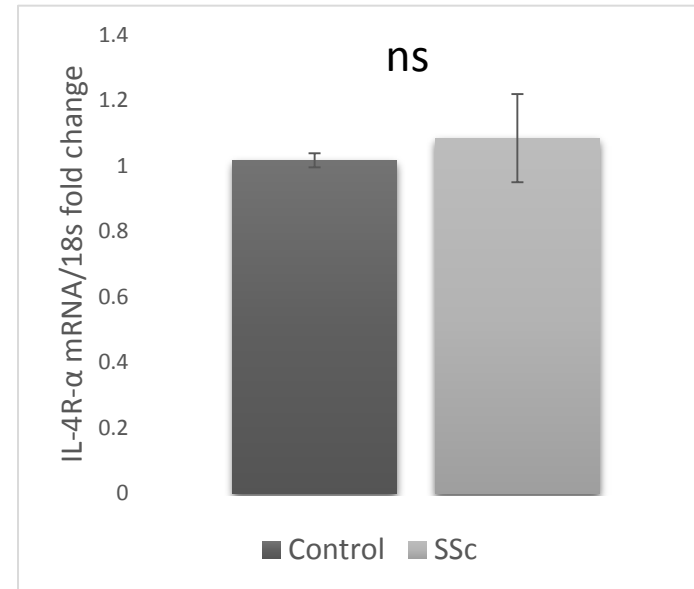
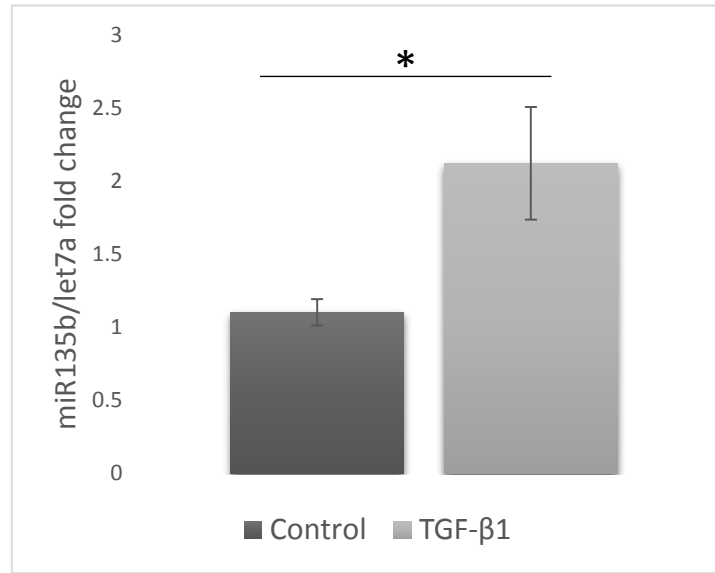
A

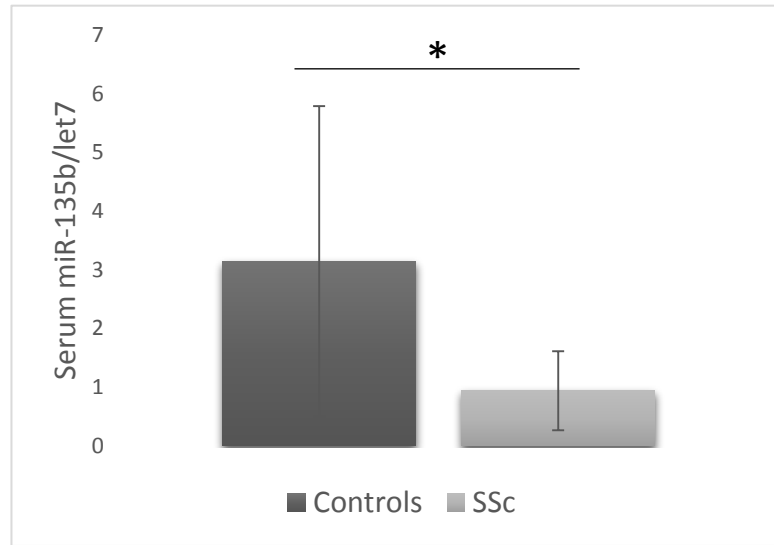
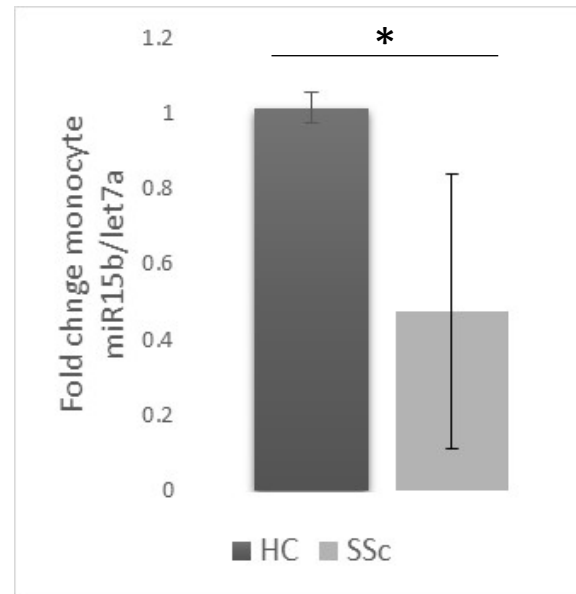
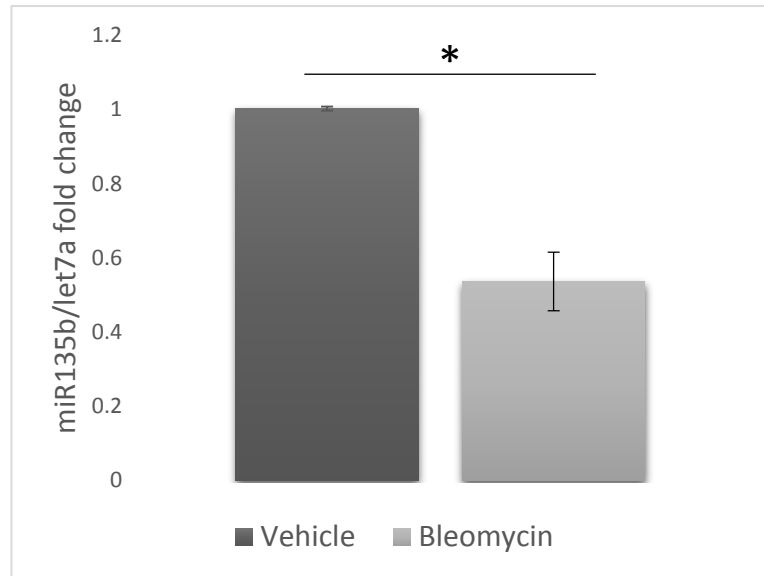
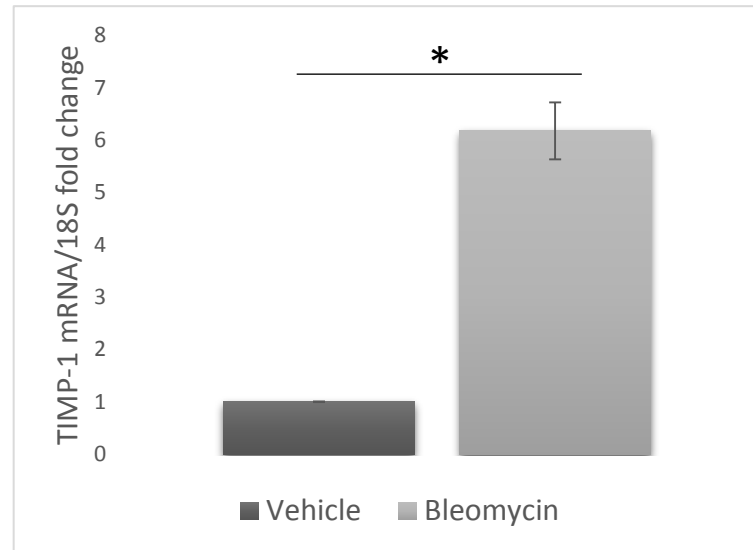


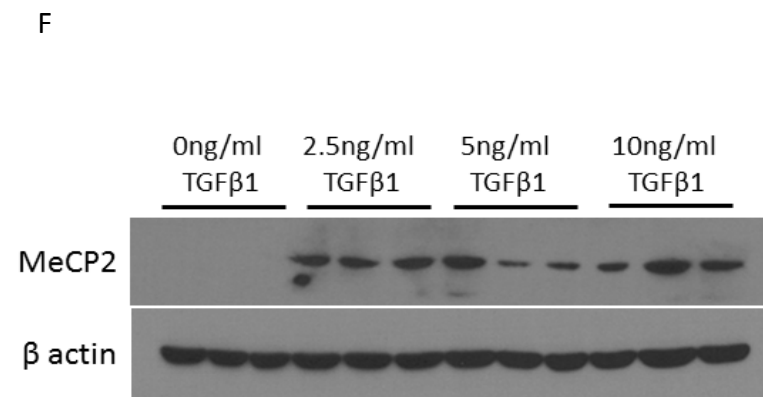
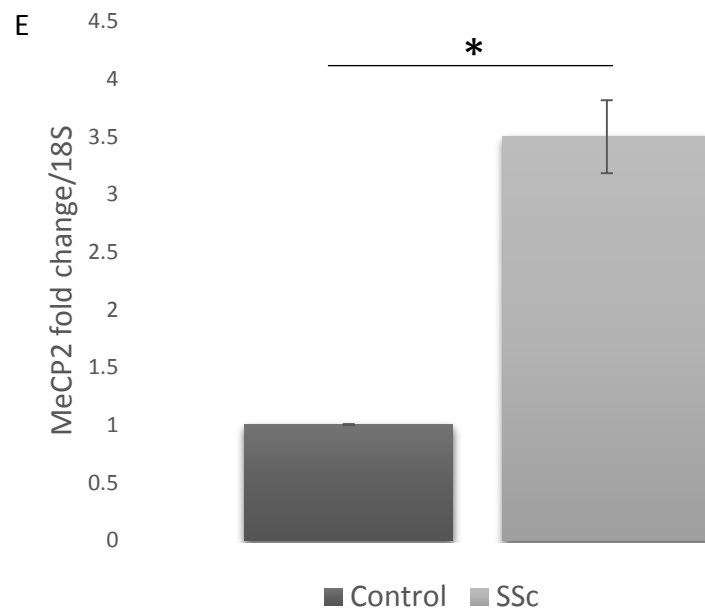
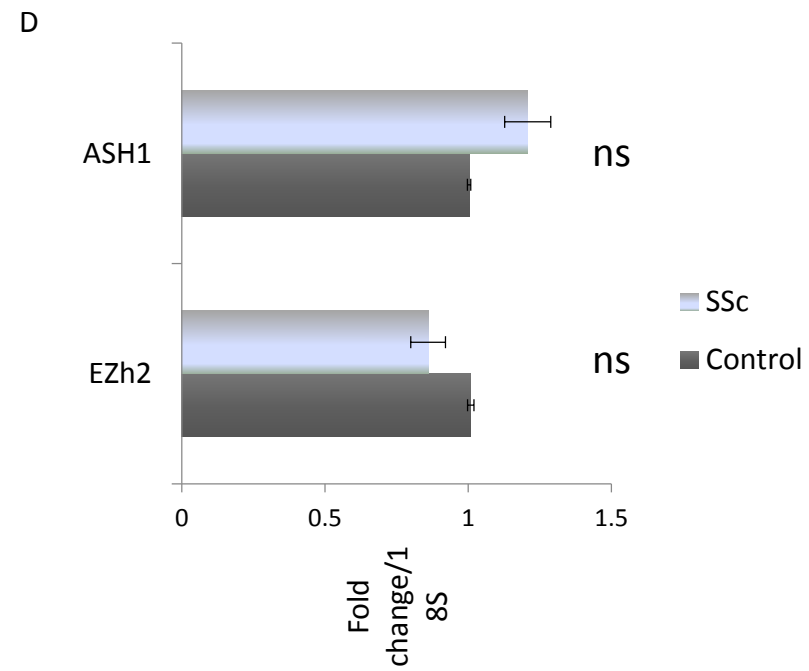
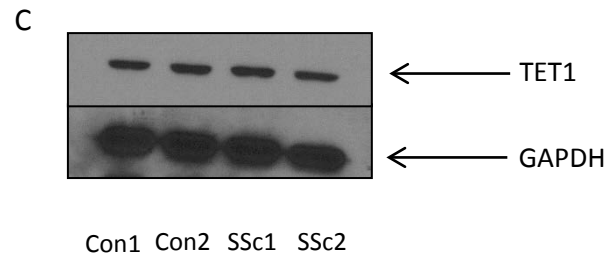
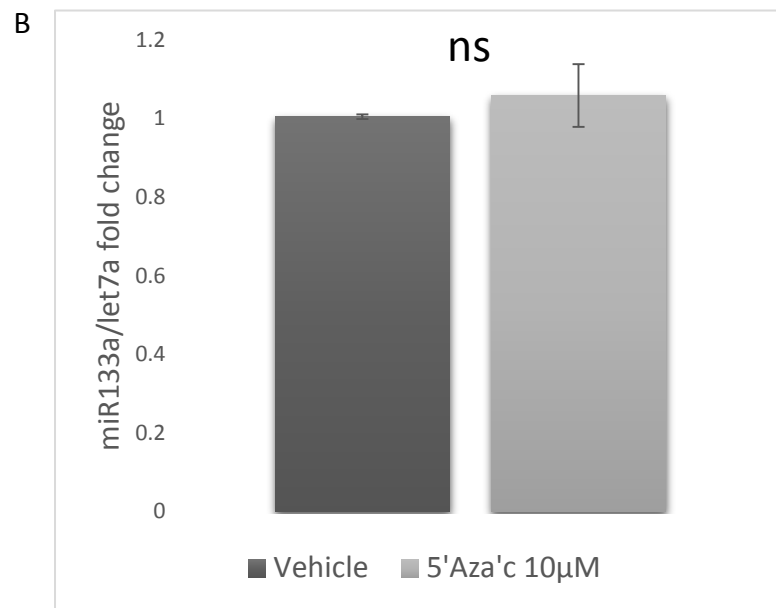
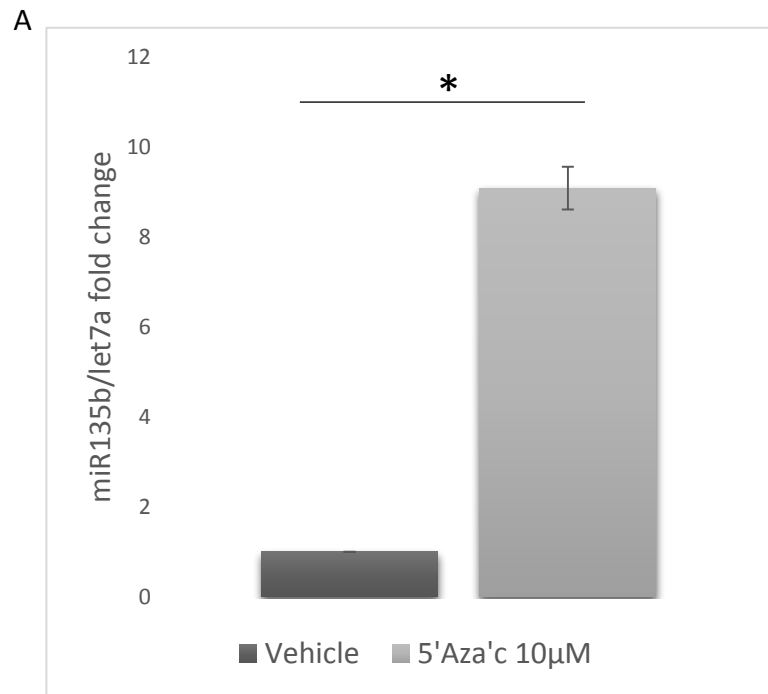
B



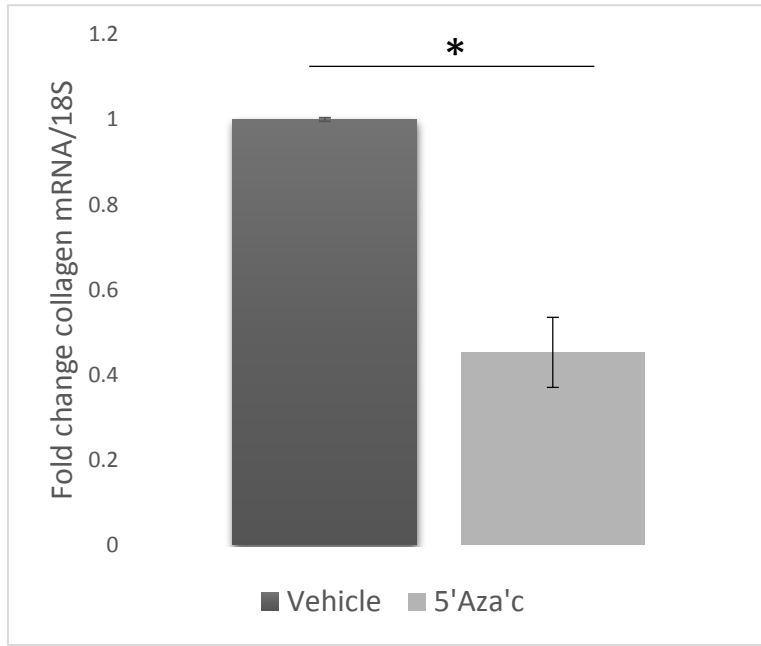
C



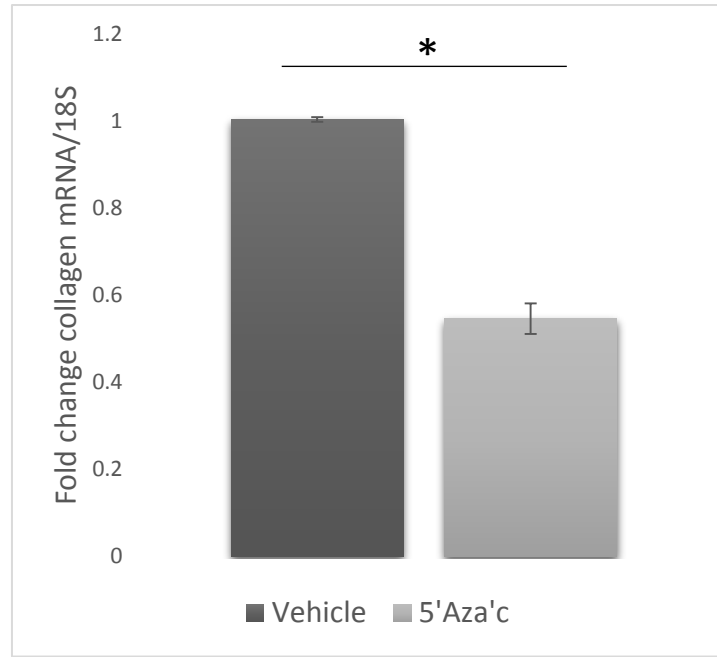
A**B****C****D**



A



B



C

